Paracrine behaviors arbitrate parasite-like interactions between tumor subclones

Robert J. Noble [1,2,3], Viola Walther [4], Christian Roumestand [5], Urszula Hibner [4,#], Michael E. Hochberg [6,7,#,*] and Patrice Lassus [4,8,*].

[1] Current: Department of Mathematics, City, University of London, London, UK.

[2] Department of Biosystems Science and Engineering, ETH Zurich, Basel, Switzerland.

[3] Department of Evolutionary Biology and Environmental Studies, University of Zurich, Zurich, Switzerland.

[4] Institut de Génétique Moléculaire de Montpellier, Univ Montpellier, CNRS, Montpellier, France

[5] Centre de Biochimie Structurale INSERM U1054, CNRS UMR 5048, Université de Montpellier, Montpellier France 34090.

[6] Institute of Evolutionary Sciences, University of Montpellier, Montpellier, France

[7] Santa Fe Institute, Santa Fe, New Mexico, USA

[8] Current: IRCM, Inserm, Univ Montpellier, ICM, CNRS, Montpellier, France

[#] These authors contributed equally to this work

* To whom correspondence should be addressed:

Patrice Lassus: patrice.lassus@inserm.fr

Michael E. Hochberg: michael.hochberg@umontpellier.fr

Abstract

Explaining the emergence and maintenance of intratumour heterogeneity is an important question in cancer biology. Tumour cells can generate considerable subclonal diversity, which influences tumour growth rate, treatment resistance and metastasis, yet we know remarkably little about how cells from different subclones interact. Here, we confronted two murine mammary cancer cell lines to determine both the nature and mechanisms of subclonal cellular interactions *in vitro.* Surprisingly, we found that compared to monoculture, growth of the 'winner' was enhanced by the presence of the 'loser' cell line, whereas growth of the latter was reduced. Our assays indicated that these interactions are mediated by the production of paracrine metabolites resulting in the winner subclone effectively 'farming' the loser. Our findings add a new level of complexity to the mechanisms underlying the subclonal growth dynamics and suggest that *in vivo* tumour interactions could be more diverse than previously thought..

Introduction

Considering tumors as complex ecosystems has led to the notion that diverse cancer cell subclones engage in heterotypic interactions reminiscent of organismal communities (Heppner, 1984; Merlo et al., 2006; Axelrod et al., 2006; Tabassum and Polyak, 2015). Positive ecological interactions (mutualism and commensalism) have been observed in cancer models in mice (Calbo et al., 2011; Cleary et al., 2014) and in drosophila (Ohsawa et al., 2012). In these cases, one subclone acquires new abilities, such as the capacity to grow or metastasize, only in the presence of another subclone, resulting in the tumor as a whole progressing towards a more aggressive phenotype.

Mutually negative interactions are thought to be ubiquitous in cancer (Nowell, 1976; Greaves & Maley, 2012). As in many ecosystems, cancer cells compete for nutrients and space, and competition between emergent subclones gives rise to complex temporal and spatial dynamics of tumor composition and growth (Tabassum and Polyak, 2015). In contrast, the prevalence within tumors of asymmetric interactions such as amensalism, parasitism and facilitation remains an open question. Defining the mechanisms of tumor ecology is essential for a better understanding of cancer progression and may lead to novel therapeutic strategies (Gatenby and Brown, 2017; Maley et al., 2017).

To gain insight into molecular and cellular events related to ecological interactions between cancer subclones, we took advantage of a model described over three decades ago, based on two closely related murine cancer cell lines derived from a single spontaneous mouse mammary tumour (Miller et al., 1988). When cultured separately, the two cell lines have similar growth rates, yet in co-culture one cell line

(the ‘winner’) expands at the expense of the other (the ‘loser’). Careful examination of this model indicated that the cellular behaviors of the two subclones are surprisingly sophisticated. Both cell lines produce paracrine metabolites that boost proliferation of the winner and also decrease the growth rate of the loser. Our results thus unveil a type of facultative parasitic behavior of the winner subclone. We further identified beta-hydroxybutyrate and lactate as metabolites that contribute to these phenotypes and characterized their modes of action. We discuss our results in the context of how previously underappreciated ecological interactions may contribute to the complexity of tumor growth dynamics.

Results

4T07 cells have a "winner" phenotype

Two cell lines derived from a single mouse mammary carcinoma - 168 and 4T07 cells - have similar growth rates when cultured individually, yet the 4T07 clone displays a dominant phenotype when grown together, either in cell culture or in orthotopic allografts *in vivo* (Miller et al., 1988). Several hypotheses to account for this interesting behavior had been tested in the original work, but the precise mechanism behind this competitive behavior has so far not been identified.

We began by verifying that in our hands the lines maintain their competitive characteristics. To facilitate lineage tracing we first generated lines stably expressing GFP, the expression of which did not alter cell growth, since all the cell lines grew at very similar rates (Figure 1A). Next, we followed growth characteristics of 4T07 and 168FARN cells, the latter being a drug-resistant derivative of the original 168 clone (Aslakson et al., 1991) in a continuous culture for 3 weeks. The cells were seeded as 1:1 mix at a density that allowed them to reach confluence within 3-4 days, at which point they were harvested and re-seeded in a new well at the original density. Remaining cells were analyzed by flow cytometry to determine the proportion of GFP expressing clones in the expanding population.

The homotypic co-culture (same line with and without GFP) confirmed that GFP has no impact on cellular proliferation (Fig1B left panels). In contrast, heterotypic co-culture conditions (two different lines, one expressing GFP) revealed the dominance of the 4T07 clone (Fig1B, right panels).

These results confirm the originally described ecological interaction between the clones: 4T07 gradually dominates the culture while the 168FARN cells become very scarce within 15-17 days. Importantly, the dominant phenotype is independent of the starting ratio between the two cell lines (Supplementary Figure 1).

Co-culture alters the proliferation rates of both "winner" and "loser" cells

As originally discussed for the two clones under study (Miller et al., 1988), the expansion of a single clone in co-culture could be due to alterations in cell death or changes in the proliferation rates of either or both clones. We measured apoptosis in the loser 168FARN clone and found identical, very low levels of cell death under homotypic and heterotypic conditions (Figure 2A). Next, we used time-lapse microscopy to assess the growth dynamics of both clones in continuous culture. The cells were at a density that reached confluence in 4 days and were photographed every 45 minutes for the last 3 days. We measured the overall pixel intensity for each frame (Figure 2B) as a proxy for the growth rate of the fluorescently tagged cell line. This analysis revealed that under co-culture conditions, the growth rate of 168FARN decreased, whereas that of 4T07 increased relative to mono-cultures. To test whether increased net growth of the winner population is due to the alteration of proliferation, we estimated the proportion of cells in the S phase of the cell cycle by performing pulse-chase EdU staining. The results presented in Figure 2C confirmed that heterotypic co-culture gave rise to significant decrease in cells actively replicating DNA for the loser clone and a significant increase in the winner clone. Overall, these results suggest that the dominant phenotype displayed by the winner cells in co-culture can be explained by changes in proliferation that operate in opposing directions on the winner and the loser cells.

β-hydroxybutyrate stimulates winner clone proliferation

To identify the molecular mechanisms at the basis of the altered growth of winners and losers when in co-culture, we first focused on the increase in proliferation rate of 4T07 cells. Heterotypic culture experiments performed at low cell density suggested that the dominant effect did not require extensive cell-cell contacts (Supplementary Figure 2). We reasoned that a soluble factor secreted by 168FARN could induce a proliferation boost in 4T07. To test this hypothesis, we collected conditioned media from each line cultured for three days and used each medium separately to grow 4T07 for an additional 24 hrs. As controls, we either left the 4T07 medium after the three days of conditioning or replaced it with fresh medium. The results shown in Figure 3A confirm our hypothesis: the medium conditioned by 168FARN induced a significant increase in 4T07 proliferation. Importantly, this effect was not due to differences of medium exhaustion by the two cell lines, since the addition of fresh medium did not boost 4T07 proliferation.

Since our data strongly suggested that a soluble factor originating from 168FARN accounted for the increase in 4T07 proliferation, we next sought to define its molecular nature. First, we separated by centrifugation the 168FARN-conditioned medium into high and low MW fractions with a 3 KDa molecular cutoff column (Sartorius). The low MW fraction contains mainly metabolites while the high one is enriched in proteins. After complementing each fraction, respectively, with 10% serum or with DMEM to obtain full media conditioned with either low or high MW secretomes, we used them in a proliferation assay as in Figure 3A. The results (Figure 3B) of this series of experiments unambiguously identified the low MW fraction of the 168FARN-conditioned medium as the source of the pro-proliferative factor. To further explore its

identity, we employed nuclear magnetic resonance spectroscopy to compare the composition of low MW fractions prepared from fresh medium and from the 168FARN- and 4T07-conditioned ones (Henke et al., 1996). Two major peaks specific for the conditioned media corresponded to a very strong signal for lactate secreted by 4T07 cells, and a significant increase in a peak identified as β-hydroxybutyrate in the 168FARN-conditioned medium (Figure 4A). β-hydroxybutyrate (BHB) is a ketone body mainly produced by the liver after long fasting periods and which is used by different tissues as a source of carbon to supplement the lack of glucose (Newman and Verdin, 2017). In addition, β-hydroxybutyrate is also produced by other cell types, such as adipocytes or cancer cells (Grabacka et al., 2016; Huang et al., 2017; Wang et al., 2017). To confirm the NMR-based identification of the β-hydroxybutyrate peak, we employed an enzymatic assay to measure β-hydroxybutyrate concentration in conditioned media from 4T07 and 168FARN (Figure 4B). The results were in perfect agreement with the NMR analysis: β-hydroxybutyrate production is significantly higher in the loser than in the winner cell clone. To test whether this metabolite was indeed responsible for the increased proliferation of 4T07, we next complemented the medium of exponentially growing 4T07 cells with purified β-hydroxybutyrate. As shown in Figure 4C, β-hydroxybutyrate increased the 4T07 proliferation rate to a level comparable to that obtained with the 168-conditioned medium. We thus conclude that loser cells increase the winner's growth rate through the secretion of β-hydroxybutyrate.

Presence of the winner clone stimulates β-hydroxybutyrate production by loser cells

After assessing β-hydroxybutyrate production in homotypic cell culture, we evaluated its secretion under heterotypic conditions. We grew 168FARN alone or together with 4T07 at a 1:1 ratio, maintaining the overall cell density constant. Surprisingly, despite the fact that under heterotypic conditions there are at least 50% fewer loser cells (which are the main producers of β-hydroxybutyrate, *cf.* Fig. 4B), the overall level of secreted β-hydroxybutyrate was higher than in the homotypic culture (Figure 4D). This suggests that either the presence of 4T07 increased the production of the metabolite by 168FARN or, alternatively, that it was 4T07 that produced more metabolite when grown in the presence of 168FARN. To distinguish between these hypotheses, we cultured both lines individually for three days, measured BHB concentration, and then exchanged the culture medium and quantified metabolite synthesis 24 hours later. The quantification of β-hydroxybutyrate produced over the last day (Day 4 BHB concentration minus Day 3 BHB concentration) shows that the 168FARN-conditioned medium had no effect on BHB secretion by 4T07 cells. In striking contrast, the production of the metabolite by 168FARN more than doubled under the influence of the 4T07-conditioned medium (Figure 4E). Thus, the winner cells stimulate the losers to produce a metabolite that boosts the former's proliferation

Mechanism of β-hydroxybutyrate action

We next asked about the mode of action of BHB on the 4T07 cells. β-hydroxybutyrate can be imported by four monocarboxylate transporters of the SLC16A gene family, the expression of which varies in different cell types. We assessed the expression of each transporter by RT-QPCR and found that MCT2, MCT3 and MCT4 were barely expressed while MCT1 is highly expressed (Figure 5A) in 4T07 cells. This result suggests that MCT1 is likely responsible for the import of β-HB in this cell line. Interestingly, we found that MCT1 is three times more expressed in 4T07 than in 168 cells (which like 4T07 do not express the other MCTs-Supplementary figure 3A) suggesting that the winner cells are more efficient at taking up this metabolite than the losers (Supplementary figure 3B). Finally, incubation of 4T07 with β-HB upregulates MCT1, consistent with a positive feedback loop that could increase the transport of this ketone body into the dominant cell line (Supplementary figure 3C).

β-hydroxybutyrate can be metabolized and used as a nutrient to replace glucose (Newman and Verdin, 2017). Experiments presented in Figure 3A show that fresh medium added at day 3 did not boost cell proliferation, suggesting that in this experimental setup the decrease in the carbon source is not a limiting factor for growth. It is thus unlikely that β-hydroxybutyrate is used as an energy resource to increase proliferation rate. β-hydroxybutyrate has previously been identified as an inhibitor of class I histone deacetylases (HDAC) that modulates the expression of genes involved in reactive oxygen species detoxification (Shimazu et al., 2013). Subsequently, another group found that adipocytes use β-hydroxybutyrate to modulate the expression of a subset of genes involved in the growth of breast cancer cells (Huang et al., 2017). We thus hypothesized that β-hydroxybutyrate might increase the growth rate of winners through the inhibition of HDACs, thereby modulating the expression of genes involved either in ROS detoxification or in the induction of pro-proliferative factors. In support of this idea, incubation of 4T07 cells either with 168FARN-conditioned medium or with purified β-HB increased H3K9 acetylation, albeit to a lesser extent than Butyrate, a bona fide HDAC inhibitor (Figure 5B).

While we could not detect in 4T07 cells any modification of expression of ROS detoxification genes reported to be regulated by β-hydroxybutyrate in other cellular models (Shimazu et al., 2013), both β-hydroxybutyrate and 168-conditioned medium led to significant transcriptional activation of interleukine 11 (IL-11) and lipocalin 2 (LCN2) (Figure 5C). Both genes have been previously described to promote cancer cell growth and to be regulated by β-hydroxybutyrate through its action on HDAC activity (Grivennikov, 2013; Huang et al., 2017; Yang and Moses, 2009). Thus, our data point to the molecular mechanisms involving direct proliferation signaling.

Lactate secretion slows down loser cell proliferation

In addition to the positive effect of the 168FARN cells on the proliferation rate of the 4T07 clone, the data shown in Figure 2 indicate that the latter negatively influences the 168FARN growth dynamics. The NMR analysis highlighted strong lactate production

(see Figure 4A). This is consistent with our observation of the media color change during culture of the two lines, indicating that the winner clone has a glycolytic type of glucose metabolism leading to a rapid medium acidification in culture. Because extracellular acidification can be detrimental for cell growth, we next asked if 168FARN were particularly sensitive to such growth conditions. We quantified medium acidification by seeding cells at different densities and measuring the extracellular pH after 3 days of culture (Figure 6A). As expected, we found that 4T07 cells acidify the medium faster and attain a lower pH during culture compared to 168FARN cells. Indeed, pH ranged from 6.94+/-0.005 (lowest density) to 6.79+/-0.003 (highest density) for the winner line and from 7.38+/-0.008 to 6.92+/-0.006 for 168FARN. To test whether 4T07-mediated extracellular acidification influenced 168FARN growth, we set up a proliferation assay for 168FARN cells grown in medium conditioned by the low and the high density grown 4T07 cells. To control for the effect of pH in the conditioned media, we included a treatment in which the medium from 4T07 was buffered at pH 7.0 by sodium bicarbonate. These experiments revealed that the medium from the low density 4T07 cells (pH 6.94) had no effect on 168FARN proliferation. In contrast, the medium from the high density 4T07 (pH 6.79) drastically decreased the 168FARN growth rate. Moreover, buffering the same medium at pH 7.0 restored the proliferative capacity of 168FARN culture. We conclude that the loser clone is more sensitive to medium acidification than the winner. Taken together our data suggest that the decrease in the growth rate of 168FARN observed in heterotypic conditions is triggered by 4T07 mediated extracellular acidification.

Discussion

Heterogeneity is a ubiquitous feature of tumors that influences growth, metastasis, and thus the potential for therapeutic success. Ecological interactions between subclones are key to the emergence of this heterogeneity, yet still only few empirical studies have characterized the nature of these interactions or their underlying mechanisms. We have shown that two cell lines derived from the same tumor exhibit a sophisticated relationship, whereby one (the 'winner') effectively farms the population of the other (the 'loser'). The signaling bases of such interactions have been previously reported (Robinson and Jordan 1999) or suggested (Marusyk et al. 2014). A recent investigation further showed that transient commensal clonal interactions can drive tumour metastasis in mice (Naffar-Abu Amara et al. 2020). Our study deepens this understanding by identifying molecules that modify interactions between cancer cell populations growing side by side.

Our *in vitro* experiments oversimplify the more complex interrelationships that predominate in spatially complex microenvironments, *in vivo*. That paracrine signaling is responsible for the effects we observed between winner and loser cell lines suggests that the spatial arrangement of these cells could be crucial to their growth and relative frequencies *in situ.* The effect of spatial structure would depend on the typical distance that secreted molecules travel through the complex tumor microenvironment. Our

results nevertheless indicate that areas of contact or close proximity between the two subclones will grow faster and therefore come to dominate spatially isolated populations, producing what is effectively a mixed 4T07-168FARN 'phenotype'. The actual spatial arrangement of these two subclones in the original tumor is unknown, but the authors of the study originally isolating these cell lines note that they may represent only a small sample of the tumor's diversity (Dexter et al., 1978). A growing body of evidence suggests that single, site-specific biopsies may be of little use in quantifying spatial heterogeneity, due to the multiscale (local, regional, metastatic) nature of tumor evolution (Amirouchene-Angelozzi et al., 2017). Computational modeling indicates that the range of cell-cell interaction and the mode of cell dispersal are crucial factors determining the pattern of intratumor heterogeneity and associated characteristics of tumor growth and evolutionary potential (Noble et al., 2020; Waclaw et al., 2015).

We find that the complex interactions between the 4T07 and 168FARN cells are governed by paracrine signaling emanating from both clones. This mechanistic conclusion differs from the original observations reported by Miller et al (Miller et al., 1988). Indeed, in the original publication the results concerning the inhibitory effect of 4T07 conditioned media on 168 cells were inconclusive. This apparent discrepancy could be due to slightly different culture conditions used in the two sets of experiments. Indeed, the medium acidification due to the lactate release by the 4T07 that is responsible for slowing down the growth of 168 cells reaches the required threshold value only after prolonged culture (3-4 days under our experimental conditions). It is thus possible that in the original report the culture time and/or the cell density were insufficient for the clear visualization of the paracrine effect of the winners on the losers. Moreover, Miller et al. did not investigate the paracrine effect exerted by the 168 on the 4T07 cells. Our results are the first to show the reciprocal effects of both cell lines on each other, thus highlighting the complexity of their mutual interactions.

We have identified a ketone body, β-hydroxybutyrate, which is produced by loser cells and acts to increase the growth rate of winner cells. Mechanistically, the competitive advantage afforded by β-hydroxybutyrate to the winner clone appears to be mediated through the HDAC-controlled activation of a genetic program that boosts its proliferation. Ketone bodies are small lipid-derived molecules, physiologically produced by the liver and distributed via the circulation to metabolically active tissues, such as muscle or brain (Newman and Verdin, 2017), where they serve as a glucose-sparing energy source in times of fasting or prolonged exercise. Recently, several studies reported that cell types such as adipocytes, intestinal stem cells or cancer cells originating from colorectal carcinoma or melanoma can also produce β-hydroxybutyrate (Cheng et al., 2019; Grabacka et al., 2016; Huang et al., 2017; Shakery et al., 2018). Our results identifying β-hydroxybutyrate as a signaling molecule involved in intra-tumoral clonal interactions fall into the general category of these novel roles for ketone bodies in cell communication.

However, the link between ketone bodies and tumor development remains controversial. On the one hand, it was shown that ketonic diet slows down tumor development in brain cancer mice models (Poff et al., 2013, 2014). On the other hand, our results together with other recent data (Huang et al., 2017) suggest that β-hydroxybutyrate may favor breast cancer progression. One unexplored possibility to explain these contradictory observations is that this ketone body can be used differently by different cancer cell types, for example as a carbohydrate supply or as a HDAC inhibitor, ultimately leading to cancer-type and context specific response.

In our experimental model, β-hydroxybutyrate increases winner cells proliferation by activating a genetic program through HDAC inhibition. Among the genes we discovered to be activated by the ketone body, IL-11 is an interleukin that displays a pro-proliferative activity (Grivennikov, 2013). Interestingly, in a distinct breast cancer cell cooperation model, sub-clonal expression of IL-11 favours the expansion not only of cells that express it, but also of other cellular sub-clones (Marusyk et al., 2014). This suggests that IL-11 acting in either paracrine or autocrine fashion could lead, respectively, to cooperation or to competition between subclones, thus participating actively in the selection and evolution of tumor heterogeneity.

Overall our experimental data therefore suggest a model in which the winner line stimulates the production of and benefits from a compound delivered by the loser line and, conversely, the loser is negatively influenced by the presence of winners through secretion of another compound.

We note that while in artificially maintained conditions of non-constrained growth (in culture) the losers are eventually eliminated, many additional selective pressures that may affect clonal fitness operate *in vivo*. These involve cellular response to physical cues due to crowding (Vishwakarma and Piddini, 2020) and interactions with the extracellular matrix (Lu et al., 2012) as well as response to signaling from the stroma, including its inflammatory and immune components (Quail and Joyce, 2013). These elements are expected to influence the outcome of the direct interactions between the tumoral clones and may change the nature of their ecological interaction from net exploitation (*in vitro*) to mutual benefit (*in vivo*). Future study should evaluate whether parasitic effects are observed *in vivo*, and determine the extent to which these cell-cell interactions mediate important tumor characteristics, including growth, drug resistance, and metastatic behavior.

Acknowledgements.

The authors wish to thank HTE 'HetCoLi' (HTE20161) and ITMO 'Physique Cancer' (CanEvolve PC201306) for funding. RN acknowledges support from the National Cancer Institute of the National Institutes of Health under Award Number U54CA217376. The content is solely the responsibility of the authors and does not necessarily represent the official views of the National Institutes of Health. CR was

supported by the French Infrastructure for Integrated Structural Biology (FRISBI) (grant No. ANR-10-INSB-05). MEH thanks the McDonnell Foundation for funding (Studying Complex Systems research award 220020294). PL and UH are grateful to Emie Quissac and Yasser Kerboua for their excellent technical assistance.

References

Amirouchene-Angelozzi, N., Swanton, C., and Bardelli, A. (2017). Tumor evolution as a therapeutic target. Cancer Discov *7*, 805–817.

Aslakson, C.J., Rak, J.W., Miller, B.E., and Miller, F.R. (1991). Differential influence of organ site on three subpopulations of a single mouse mammary tumor at two distinct steps in metastasis. International Journal of Cancer *47*, 466–472.

Axelrod, R., Axelrod, D.E., and Pienta, K.J. (2006). Evolution of cooperation among tumor cells. Proceedings of the National Academy of Sciences of the United States of America *103*, 13474–13479.

Cairns, J. (1975). Mutation selection and the natural history of cancer. Nature *255*, 197–200.

Calbo, J., van Montfort, E., Proost, N., van Drunen, E., Beverloo, H.B., Meuwissen, R., and Berns, A. (2011). A functional role for tumor cell heterogeneity in a mouse model of small cell lung cancer. Cancer Cell *19*, 244–256.

Cheng, C.-W., Biton, M., Haber, A.L., Gunduz, N., Eng, G., Gaynor, L.T., Tripathi, S., Calibasi-Kocal, G., Rickelt, S., Butty, V.L., et al. (2019). Ketone Body Signaling Mediates Intestinal Stem Cell Homeostasis and Adaptation to Diet. Cell *178*, 1115-1131.e15.

Cleary, A.S., Leonard, T.L., Gestl, S.A., and Gunther, E.J. (2014). Tumour cell heterogeneity maintained by cooperating subclones in Wnt-driven mammary cancers. Nature *508*, 113–117.

Dexter, D.L., Kowalski, H.M., Blazar, B.A., Fligiel, Z., Vogel, R., and Heppner, G.H. (1978). Heterogeneity of tumor cells from a single mouse mammary tumor. Cancer Research *38*, 3174–3181.

Gatenby, R.A., and Brown, J. (2017). Mutations, evolution and the central role of a self-defined fitness function in the initiation and progression of cancer. Biochimica et Biophysica Acta (BBA) - Reviews on Cancer *1867*, 162–166.

Grabacka, M.M., Wilk, A., Antonczyk, A., Banks, P., Walczyk-Tytko, E., Dean, M., Pierzchalska, M., and Reiss, K. (2016a). Fenofibrate Induces Ketone Body Production in Melanoma and Glioblastoma Cells. Frontiers in Endocrinology *7*.

Grabacka, M.M., Wilk, A., Antonczyk, A., Banks, P., Walczyk-Tytko, E., Dean, M., Pierzchalska, M., and Reiss, K. (2016b). Fenofibrate Induces Ketone Body

Production in Melanoma and Glioblastoma Cells. Frontiers in Endocrinology *7*, 5.

Greaves, M., and Maley, C.C. (2012). Clonal evolution in cancer. Nature *481*, 306–313.

Grivennikov, S.I. (2013). IL-11: a prominent pro-tumorigenic member of the IL-6 family. Cancer Cell *24*, 145–147.

Henke, J., Willker, W., Engelmann, J., and Leibfritz, D. (1996). Combined extraction techniques of tumour cells and lipid/phospholipid assignment by two dimensional NMR spectroscopy. Anticancer Research *16*, 1417–1427.

Heppner, G. H. (1984). Tumor heterogeneity. Cancer Research *44*, 2259–2265.

Huang, C.-K., Chang, P.-H., Kuo, W.-H., Chen, C.-L., Jeng, Y.-M., Chang, K.-J., Shew, J.-Y., Hu, C.-M., and Lee, W.-H. (2017). Adipocytes promote malignant growth of breast tumours with monocarboxylate transporter 2 expression via β-hydroxybutyrate. Nature Communications *8*, 14706.

Lu, P., Weaver, V.M., and Werb, Z. (2012). The extracellular matrix: A dynamic niche in cancer progression. J. Cell Biol.

Maley, C.C., Aktipis, A., Graham, T.A., Sottoriva, A., Boddy, A.M., Janiszewska, M., Silva, A.S., Gerlinger, M., Yuan, Y., Pienta, K.J., et al. (2017). Classifying the evolutionary and ecological features of neoplasms. Nature Reviews Cancer *17*, 605–619.

Marusyk, A., Almendro, V., and Polyak, K. (2012). Intra-tumour heterogeneity: a looking glass for cancer? Nature Reviews Cancer *12*, 323–334.

Marusyk, A., Tabassum, D.P., Altrock, P.M., Almendro, V., Michor, F., and Polyak, K. (2014). Non-cell-autonomous driving of tumour growth supports sub-clonal heterogeneity. Nature *514*, 54–58.

Merlo, L.M.F., Pepper, J.W., Reid, B.J., and Maley, C.C. (2006). Cancer as an evolutionary and ecological process. Nature Reviews Cancer *6*, 924–935.

Miller, B.E., Miller, F.R., Wilburn, D., and Heppner, G.H. (1988). Dominance of a tumor subpopulation line in mixed heterogeneous mouse mammary tumors. Cancer Research *48*, 5747–5753.

Naffar-Abu Amara, S., Kuiken, H. J., Selfors, L. M., Butler, T., Leung, M. L., Leung, C. T., … Brugge, J. S. (2020). Transient commensal clonal interactions can drive tumor metastasis. Nature Communications, *11*(1).

Newman, J.C., and Verdin, E. (2017). β-Hydroxybutyrate: A Signaling Metabolite. Annual Review of Nutrition *37*, 51–76.

Noble, R., Burley, J.T., Le Sueur, C., and Hochberg, M.E. (2020). When, why and how tumour clonal diversity predicts survival. Evol. Appl *13*, 1558–1568.

Nowell, P. (1976). The clonal evolution of tumor cell populations. Science *194*, 23–28.

Ohsawa, S., Sato, Y., Enomoto, M., Nakamura, M., Betsumiya, A., and Igaki, T. (2012). Mitochondrial defect drives non-autonomous tumour progression through Hippo signalling in Drosophila. Nature *490*, 547–551.

Poff, A.M., Ari, C., Seyfried, T.N., and D'Agostino, D.P. (2013). The ketogenic diet and hyperbaric oxygen therapy prolong survival in mice with systemic metastatic cancer. PloS One *8*, e65522.

Poff, A.M., Ari, C., Arnold, P., Seyfried, T.N., and D'Agostino, D.P. (2014). Ketone supplementation decreases tumor cell viability and prolongs survival of mice with metastatic cancer. International Journal of Cancer *135*, 1711–1720.

Quail, D.F., and Joyce, J.A. (2013). Microenvironmental regulation of tumor progression and metastasis. Nat. Med *19*, 1423–1437.

Shakery, A., Pourvali, katayoun, Ghorbani, A., Sadat Fereidani, S., and Zand, H. (2018). Beta-Hydroxybutyrate Promotes Proliferation, Migration and Stemness in a Subpopulation of 5FU Treated SW480 Cells: Evidence for Metabolic Plasticity in Colon Cancer. Asian Pacific Journal of Cancer Prevention *19*, 3287–3294.

Shimazu, T., Hirschey, M.D., Newman, J., He, W., Shirakawa, K., Le Moan, N., Grueter, C.A., Lim, H., Saunders, L.R., Stevens, R.D., et al. (2013). Suppression of oxidative stress by β-hydroxybutyrate, an endogenous histone deacetylase inhibitor. Science (New York, N.Y.) *339*, 211–214.

Tabassum, D.P., and Polyak, K. (2015). Tumorigenesis: it takes a village. Nature Reviews Cancer *15*, 473–483.

Vishwakarma, M., and Piddini, E. (2020). Outcompeting cancer. Nat. Rev. Cancer *20*, 187–198.

Waclaw, B., Bozic, I., Pittman, M.E., Hruban, R.H., Vogelstein, B., and Nowak, M.A. (2015). A spatial model predicts that dispersal and cell turnover limit intratumour heterogeneity. Nature *525*, 261–264.

Wang, Q., Zhou, Y., Rychahou, P., Fan, T.W.-M., Lane, A.N., Weiss, H.L., and Evers, B.M. (2017). Ketogenesis contributes to intestinal cell differentiation. Cell Death & Differentiation *24*, 458–468.

Yang, J., and Moses, M.A. (2009). Lipocalin 2: A multifaceted modulator of human cancer. Cell Cycle *8*, 2347–2352.

Figure Legends

Figure 1 Mutual impacts on subclonal growth

A: 168FARN and 4T07 parental cells were transduced either with an empty retroviral vector(168P and 4T07P) or with labelled with a GFP-encoding retrovirus (168G and 4T07G). Cells were seeded in triplicate in 6-well plates at a density of 50 000 cells/well

and cultured for the indicated times before harvesting and counting. **B:** 10^5 cells were seeded at a 1:1 ratio in homotypic (parental and GFP expressing derivative of the same cell line) or heterotypic (different cell lines, one expressing GFP) co-cultures and harvested and replated as indicated. The ratios of GFP to unlabelled cells were estimated by flow cytometry. The results represent data from 3 independent experiments.

Figure 2. Heterotypic co-culture alters the proliferation kinetics of both winner and loser cell lines

A: A total of 10^5 cells were seeded. 168G cells were co-cultured with either the 168P (homotypic) or 4T07P (heterotypic) cells at a 1:1 ratio for 4 days and harvested. Apoptosis was quantified by flow cytometry following Annexin-V staining. **B:** Homo- and heterotypic mixes of subclones were seeded at the density 10^5 cells per well at a 1:1 ratio, as indicated. The growth was assessed by time-lapse microscopy. The GFP fluorescence gave the measure of expansion of the labeled subclone. The data from three independent experiments were normalized by setting initial fluorescence to an arbitrary value of 1. Mean values from all experiments are presented. **C:** Cells grown in homo- and hetreotypic co-cultures as in **A**. Before harvesting at day 4 cells were labelled by a 2hr pulse of EdU and the fraction of cells in the S phase was determined by flow cytometry. ns: not significant, * $p<0.05$, ** $p<0.01$

Figure 3. Soluble factor secreted by 168FARN cells accelerates proliferation of the 4T07 cells

A: 4T07 cells were grown for 3 days at which point their medium was either left unchanged, or replaced by 168FARN-conditioned medium or fresh medium, as indicated. Cells were collected 24 hrs later and counted. Cell numbers at day 3 were arbitrarily set at 1 in order to include the data from 3 independent experiments. **B:** The experiment was performed as in **A.** but the medium conditioned by 168FARN cells was fractionated by membrane ultrafiltration with a 3 KDa molecular cutoff. After complementing the low and the high MW fractions, respectively, with 10% serum and DMEM, the media were used to grow the 4T07 cells, as in **A**. The two fractions were also combined as a control.. ns: not significant, * $p<0.05$, ** $p<0.01$, *** $p<0.001$, all compared to Day 4 point.

Figure 4. Identification of soluble metabolites altering the heterotypic growth dynamics .

A: Superimposition of the high-field region of representative 1D proton NMR spectra recorded at 700 MHz, 293 K and pH7 on samples of culture media collected after growing 40T7 cells (1) or 168FARN cells (2) for 3 days or of fresh cell culture medium (3). The arrows indicate the characteristic resonance of Lactate and β-hydroxybutyrate.

The insert displays a zoom in this spectral region, revealing the H-alpha resonance of the β-hydroxybutyrate. For all spectra, peak intensities have been normalized on the intensity of the DSS resonance added as internal reference. **B:** Concentration of β-hydroxybutyrate from fresh medium and from conditioned medium from 168FARN or 4T07 was quantified by enzymatic reaction. **C:** Commercially available β-hydroxybutyrate at indicated concentrations was added to 4T07 cell culture at day 3 an the growth allowed to proceed for an additional 24 hrs **D:** 168FARN alone (homotypic) or in 1:1 co-culture with 4T01 cells were grown for 4 days and extracellular β-hydroxybutyrate was measured enzymatically as in 4B. **E:** 168FARN and 4T07 cells were cultured individually for 3 days. The medium was then replaced by the homotypic or heterotypic conditioned one, as indicated, and the culture allowed to continue for an additional 24 hrs. The β- hydroxybutyrate concentration was quantified at day 4.

Figure 5 Extracellular β-hydroxybutyrate leads to increased H3K9 histone acetylation and altered gene expression in 4T07 cells

A: Expression levels of the slc16A family transporter genes in 4T07 were analyzed by RT-QPCR. Expression of HPRT served as normalization of the data. **B:** H3K9 histone acetylation was analyzed by immunblotting of extracts of 4T07 cells grown for 24 hrs in control, 168-conditioned medium or medium complemented with β-hydroxybutyrate or with butyrate, as indicated. **C:** 4T07 cells cultured for 3 days were incubated for 8 hours with 4T07- (Ctrl) or 168- conditioned medium or purified β-hydroxybutyrate (10mM). Total RNAs were purified and subjected to RT-QPCR with specific primers for LCN2 and IL-11.

Figure 6 Impact of extracellular pH on the loser clone growth.

A: 168FARN and 4T07 cells were seeded at the indicated initial densities in 6-well plates and cultured for 3 days. Culture media were removed, immediately covered with a layer of mineral oil to prevent oxidation and the pH was measured. **B:** 10^5 168FARN cells were grown for 3 days. Medium was then replaced by conditioned media from cultures grown at low or high density, as indicated. Where indicated, 5mM $NaCO_3$ was used to buffer the 4T07 conditioned medium to pH7. 24 hours later cells were harvested and counted. Data are from three independent experiments conducted in triplicates.

Supplementary Figure 1

A and B: Growth dynamics of subclones under homotypic and heterotypic conditions. Experiments were performed as in Figure 2B. Starting ratio was 1:4 in A and 3:1 % in B.

Supplementary Figure 2

A: Growth dynamics of subclones at low and high density. Experiments were performed as in Figure 2B. Cells were grown in heterotypic conditions at a starting ratio of 1:1. Cells were seeded either at low density (50K) or high density (150k), diluted and quantified every 3 days. At low density, cells never reached confluency on day 3.

Supplementary Figure 3

A: ***Expression levels of the slc16A family transporter genes in 168FARN*** **.** RT-QPCR analysis was performed on 168FARN RNA for Mct2, Mct1, Mct3 and Mct4 genes and normalized to HPRT. Relative expression levels were compared to Mct2**B: Slc16A1 expression in both subclones.** Slc16A1 RNA levels were monitored by RT-QPCR, normalized with HPRT and adjusted relative to levels in 168FARN cells cells. **B: Influence of Slc16A1 expression by β-hydroxybutyrate.** Experiment was performed as in Figure 5B. Slc16A1 RNA levels were quantified as in A and adjusted relative to levels in control condition.

Methods

Cell culture

4T07 and 168FARN were a kind gift of Dr Robert Hipskind. All cell lines were cultured in Dulbecco's modified Eagle medium containing 10% fetal bovine serum, 100 ng/mL streptomycin, and 100 U/mL penicillin at 37 ºC with 5% CO2.

For co-culture experiments a mixture of GFP-labelled and parental cells (empty-vector transduced) cells were seeded at the final density of 10^5 cells/well in 6-well plates except mentioned otherwise. Upon reaching confluence (3-4 days) they were harvested, diluted to the original density and replated. The remaining fraction was analyzed by flow cytometry.

Immunoblot Analysis

Cells were lysed in boiling Laemmli buffer supplemented with protease inhibitors, then sonicated and complemented with DTT. Protein concentration was determined by BCA (Thermo Scientific) assay. Fifteen to twenty micrograms of total protein were loaded onto SDS-PAGE gels and transferred onto nitrocellulose membranes. The membrane

was blocked with TBST (1× TBS with 0.1% Tween 20) + 5% milk at room temperature for 1 h and incubated with primary antibody and then with horseradish peroxidase (HRP)-coupled secondary antibody (Amersham, Piscataway, NJ). Activity was visualized by electrochemiluminescence. Antibodies used in this study are anti Histone H3 (Cell signaling Technology #9717) and anti- Acetyl-Histone H3 (Lys9) (Cell signaling Technology #9649).

Reverse Transcription and Real-Time PCR

Total mRNA was isolated using a RNeasy mini kit (Qiagen, Germantown, MD, USA). Reverse transcription was performed with random hexamers and M-MLV Reverse Transcriptase (Invitrogen). Real-time PCR was performed in triplicates with LC FastStart DNA Master SYBR Green I on a LightCycler rapid thermal cycler system (Roche Diagnostics, Mannheim, Germany), according to the manufacturer's instructions. Housekeeping gene HPRT was used for normalization. Primers sequences are available upon request.

Time-lapse microscopy

Time-lapse microscopy was performed at 37 ºC with 5% CO2, with images taken at 45-minute intervals using an inverted Zeiss Axio-Observer microscope. The images were processed and analyzed using ImageJ software.

EdU staining

Cells were incubated with 10μM EdU for 2 hours, harvested and processed using the Click-iT™ EdU Alexa Fluor™ 647 Flow Cytometry Assay Kit (ThermoFisher Scientific #C10424) following manufacturer instructions. Labeled cells were then analyzed on a FACSCalibur flow cytometer using CellQuestPro software (BD Biosciences).

Apoptosis quantification

To determine the percentage of apoptotic cells with externalized phosphatidylserine (PS), adherent and floating cells were collected and labeled with the Annexin V-Cy3 Apoptosis Detection Kit (Abcam, Cambridge, UK, #ab14143) according to the manufacturer's instructions. Labeled cells were then analyzed on a FACSCalibur flow cytometer using CellQuestPro software (BD Biosciences).

β-hydroxybutyrate quantification

β-hydroxybutyrate concentration was measured by an enzymatic kit (Sigma-Aldrich MAK041) following the manufacturer instructions. Briefly, β-hydroxybutyrate present in the culture medium was determined by a coupled enzyme reaction, resulting in a

colorimetric (450 nm) product, proportional to the β-hydroxybutyrate concentration. The absorbance was measured on a spectrophotometer.

RMN analysis

NMR experiments were recorded at 293K and pH 7 on an AVANCE III BRUKER spectometer operating at 700 MHz (proton frequency), using a Z-gradient shielded TCI 1H-13C-15N cryoprobe. Fully relaxed 1D 1H spectra were aquired with the regular 1D NOESY, using 5s as relaxation delay. The samples consisted on 1.5 mL of cell media (fresh or conditioned by cell culture), lyophilized and dissolved in 500 µL of deuterated phosphate buffer (50 mM, pH 7). DSS (EURISOTOP©, final concentration: 0.5 mM) was added as internal reference for chemical shift referencing and as a concentration standard for spectra normalization. The assignment of the 1H resonances of the compound of interest in this study (Lactate, β-hydroxybutyrate) was based on chemical shifts reported on the litterature (1) and further confirmed using 2D [1H,1H] (TOCSY) and [1H-13C] (HSQC, HSQC-TOCSY) NMR spectroscopy.

Statistical analysis

Experiments were repeated at least three times. Data are presented as mean ± SEM. An Independent Student's t test was performed to analyze the assay results; a two-tailed Student's t test was used to compare the intergroup differences. Significance was accepted for values where $P \leq 0.05$ (*), $P \leq 0.01$ (**), $P \leq 0.001$ (***).

Figure 1

A

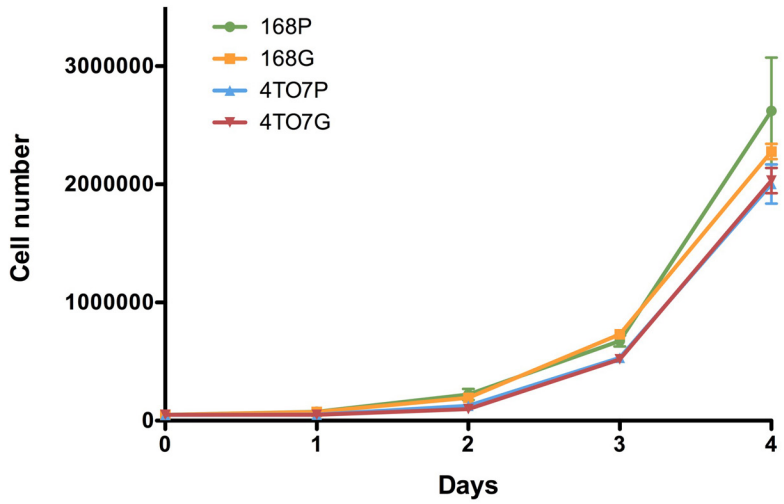
168P
168G
4TO7P
4TO7G
Cell number
3000000
2000000
1000000
0
0
1
2
3
4
Days

B

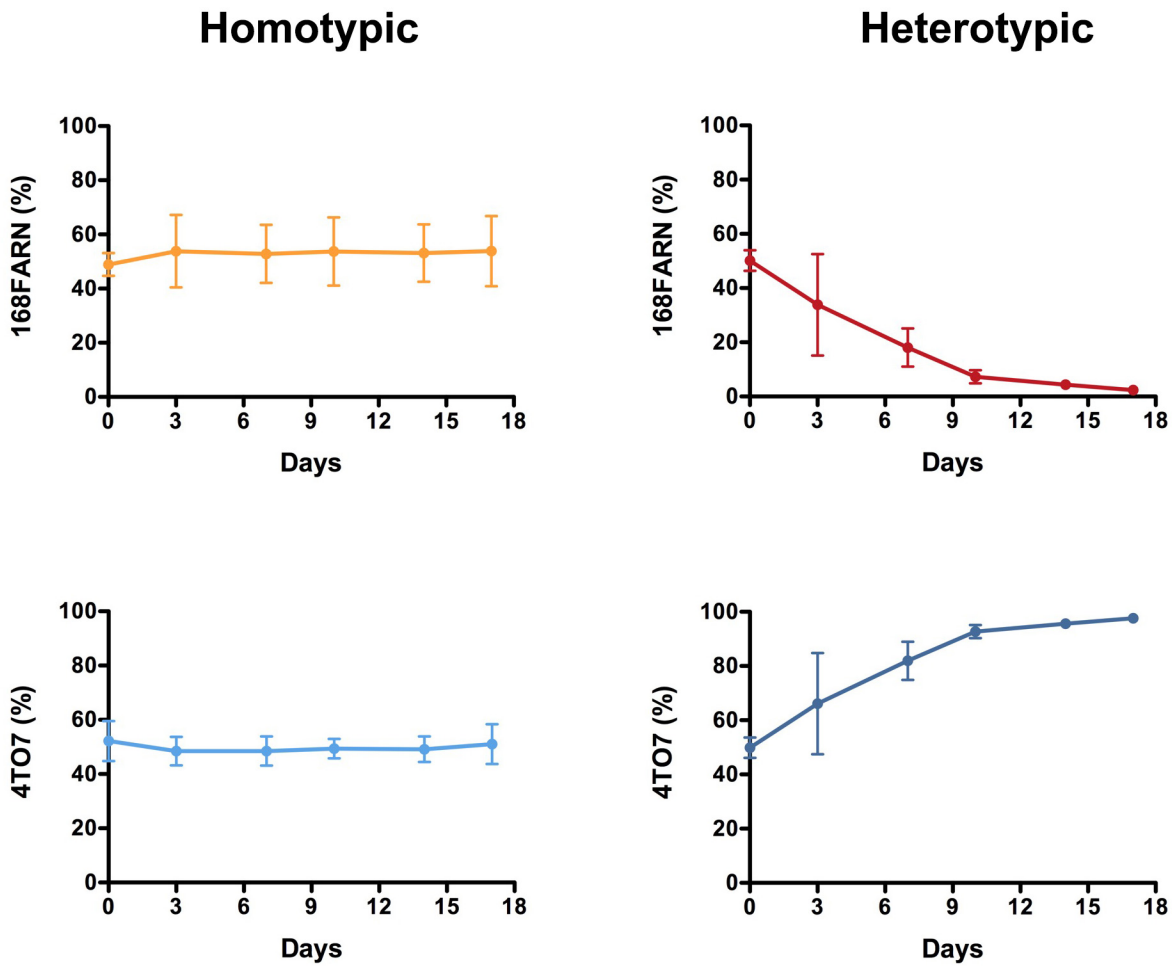
Homotypic
Heterotypic
168FARN (%)
4TO7 (%)
100
80
60
40
20
0
0
3
6
9
12
15
18
Days

Figure 2

A

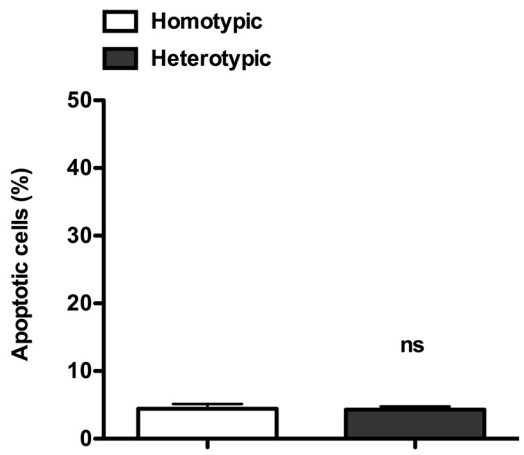
Homotypic
Heterotypic
Apoptotic cells (%)
50
40
30
20
10
0
ns

B

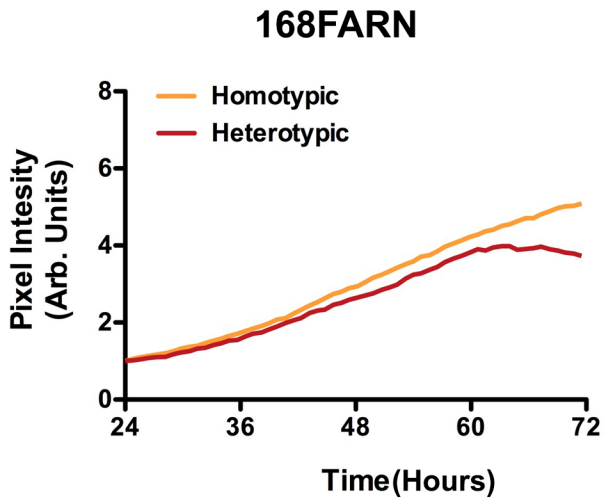
168FARN
Homotypic
Heterotypic
Pixel Intesity (Arb. Units)
8
6
4
2
0
24
36
48
60
72
Time(Hours)

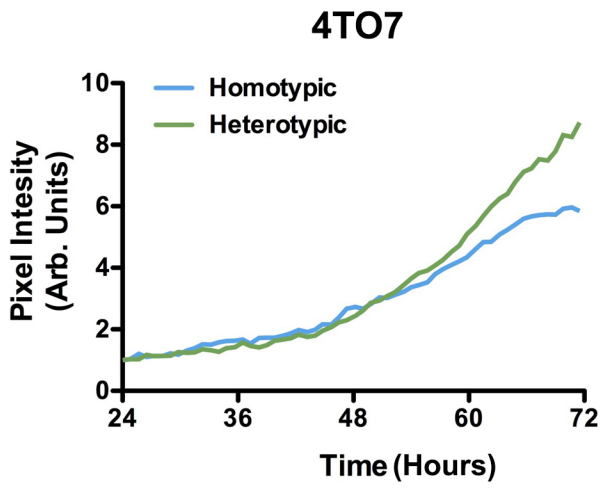
4TO7
Homotypic
Heterotypic
Pixel Intesity (Arb. Units)
10
8
6
4
2
0
24
36
48
60
72
Time (Hours)

C

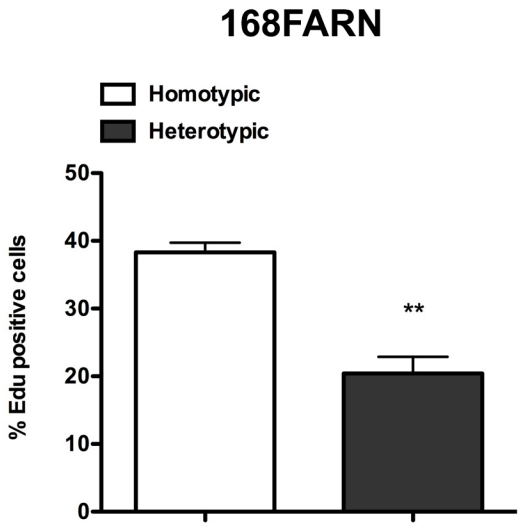
168FARN
Homotypic
Heterotypic
% Edu positive cells
50
40
30
20
10
0
**

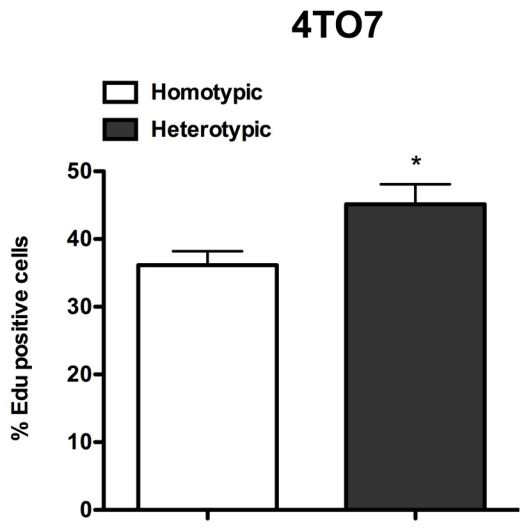
4TO7
Homotypic
Heterotypic
% Edu positive cells
50
40
30
20
10
0
*

Figure 3

A

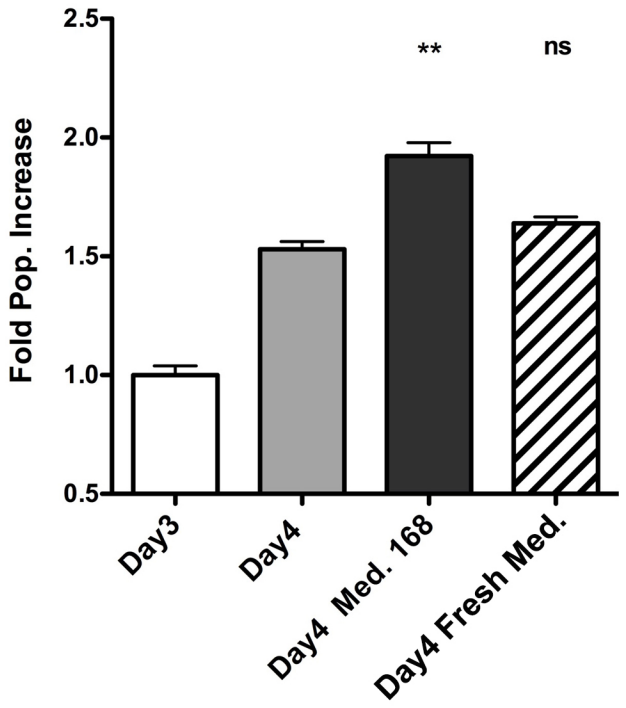
2.5
2.0
1.5
1.0
0.5
Fold Pop. Increase
**
ns
Day3
Day4
Day4 Med. 168
Day4 Fresh Med.

B

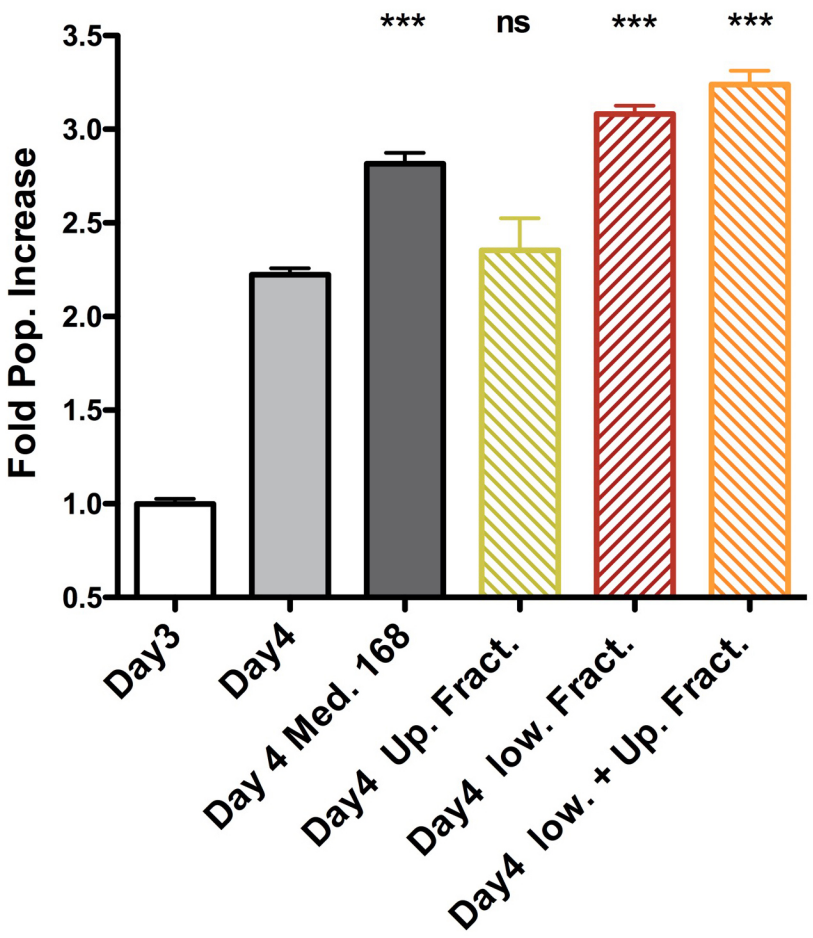
3.5
3.0
2.5
2.0
1.5
1.0
0.5
Fold Pop. Increase
***
ns
***
***
Day3
Day4
Day 4 Med. 168
Day4 Up. Fract.
Day4 low. Fract.
Day4 low. + Up. Fract.

Figure 4

A

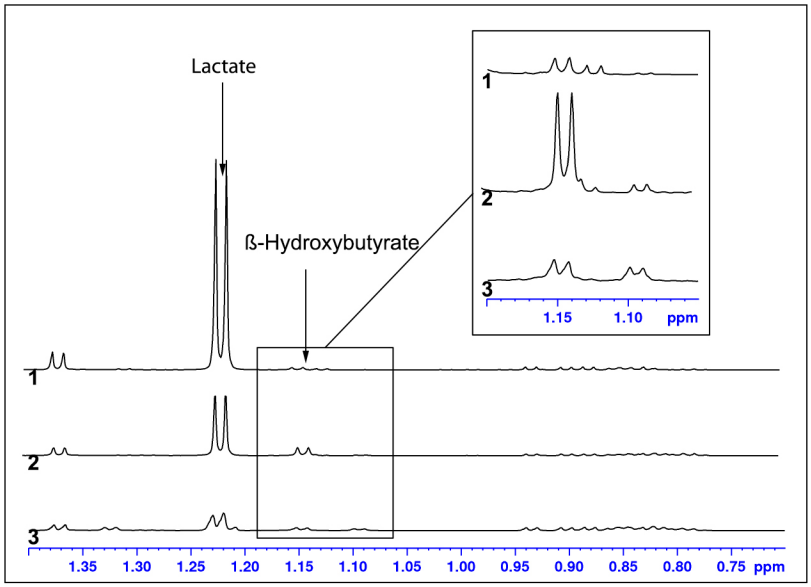

B

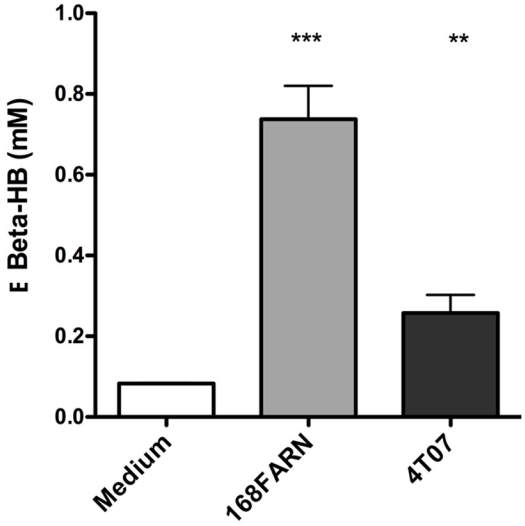

C

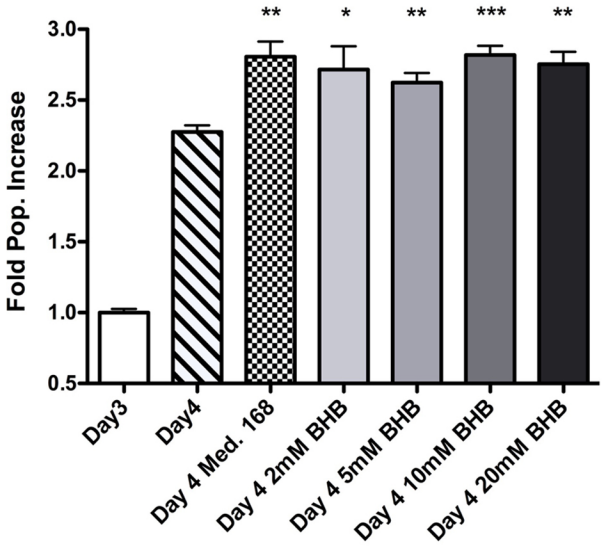

D

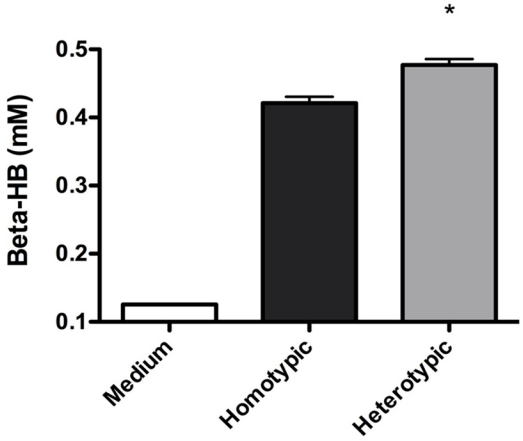

E

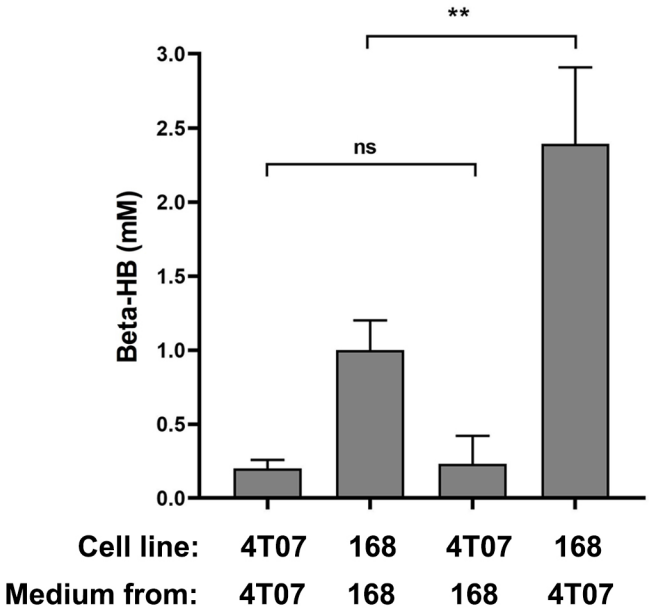

Figure 5

A

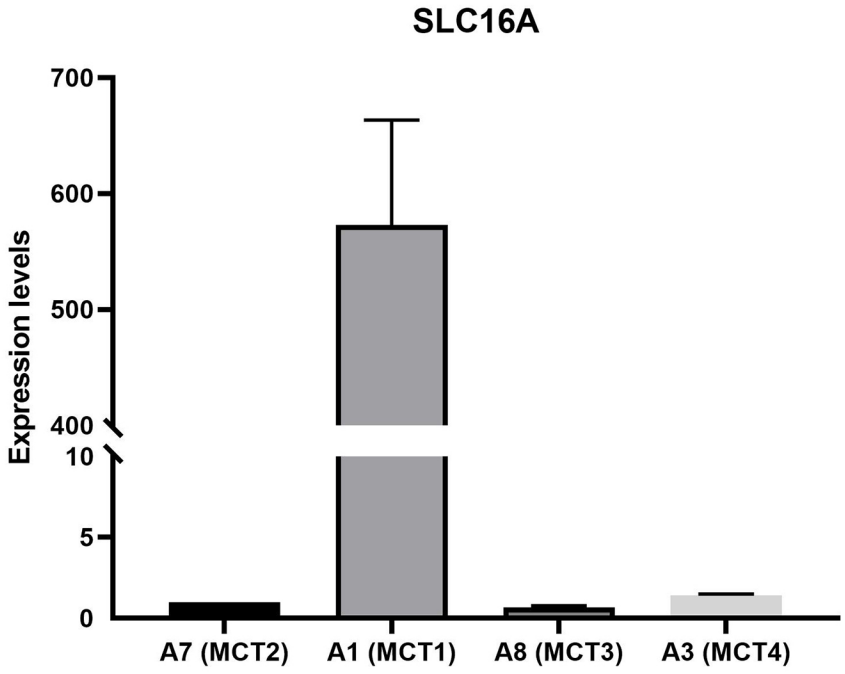
SLC16A
Expression levels
700
600
500
400
10
5
0
A7 (MCT2)
A1 (MCT1)
A8 (MCT3)
A3 (MCT4)

B

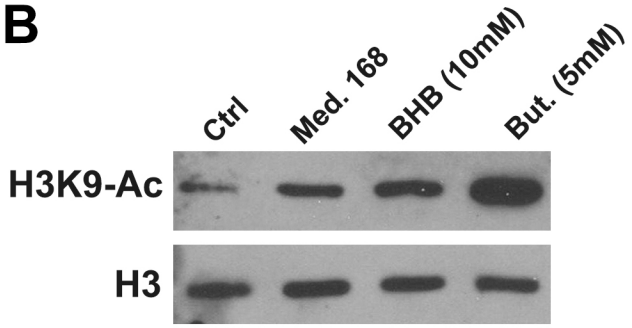
Ctrl
Med. 168
BHB (10mM)
But. (5mM)
H3K9-Ac
H3

C

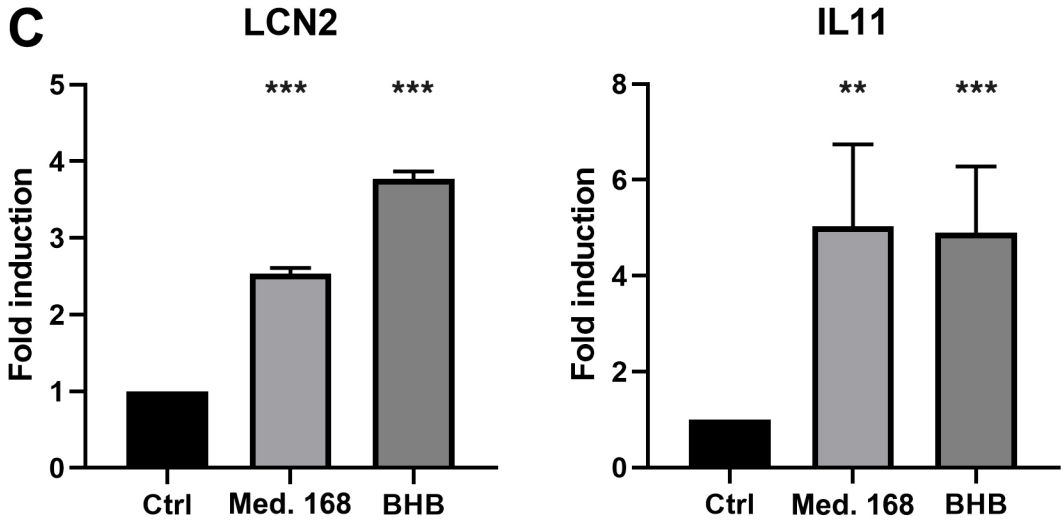
LCN2
IL11
Fold induction
***
***
**
***
Ctrl
Med. 168
BHB

Figure 6

A

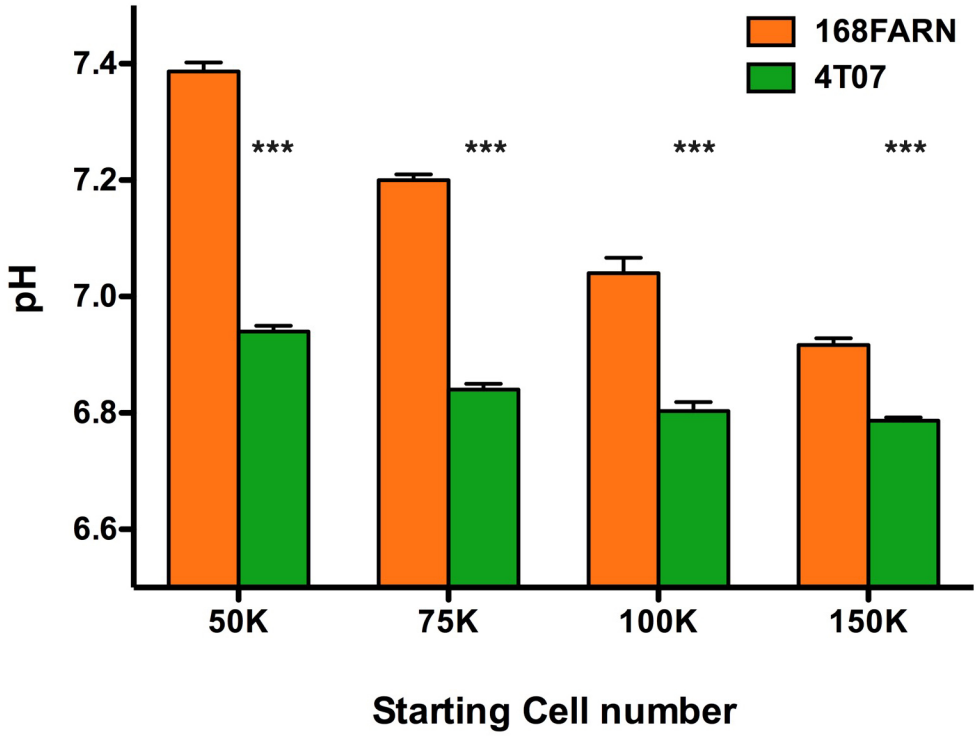
168FARN
4T07
pH
7.4
7.2
7.0
6.8
6.6
***
***
***
***
50K
75K
100K
150K
Starting Cell number

B

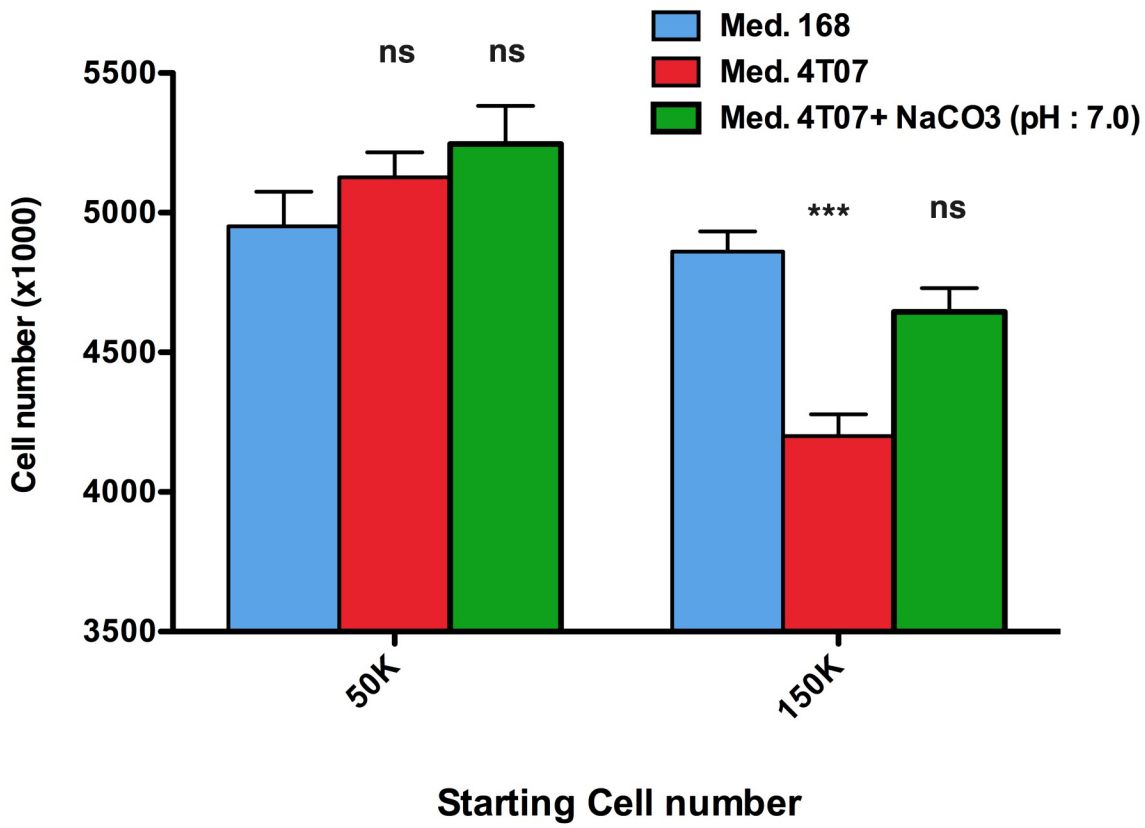
Med. 168
Med. 4T07
Med. 4T07+ NaCO3 (pH : 7.0)
Cell number (x1000)
5500
5000
4500
4000
3500
ns
ns
***
ns
50K
150K
Starting Cell number

Supplementary Figure 1

A

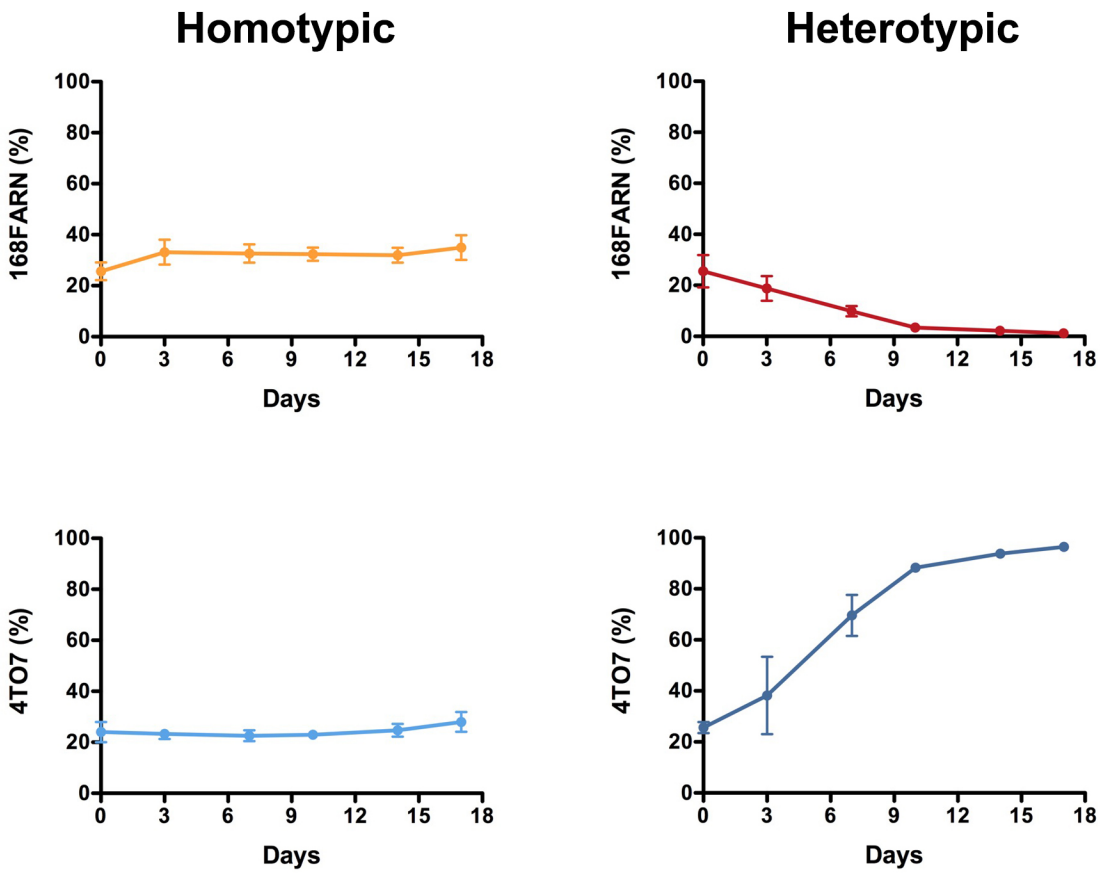

B

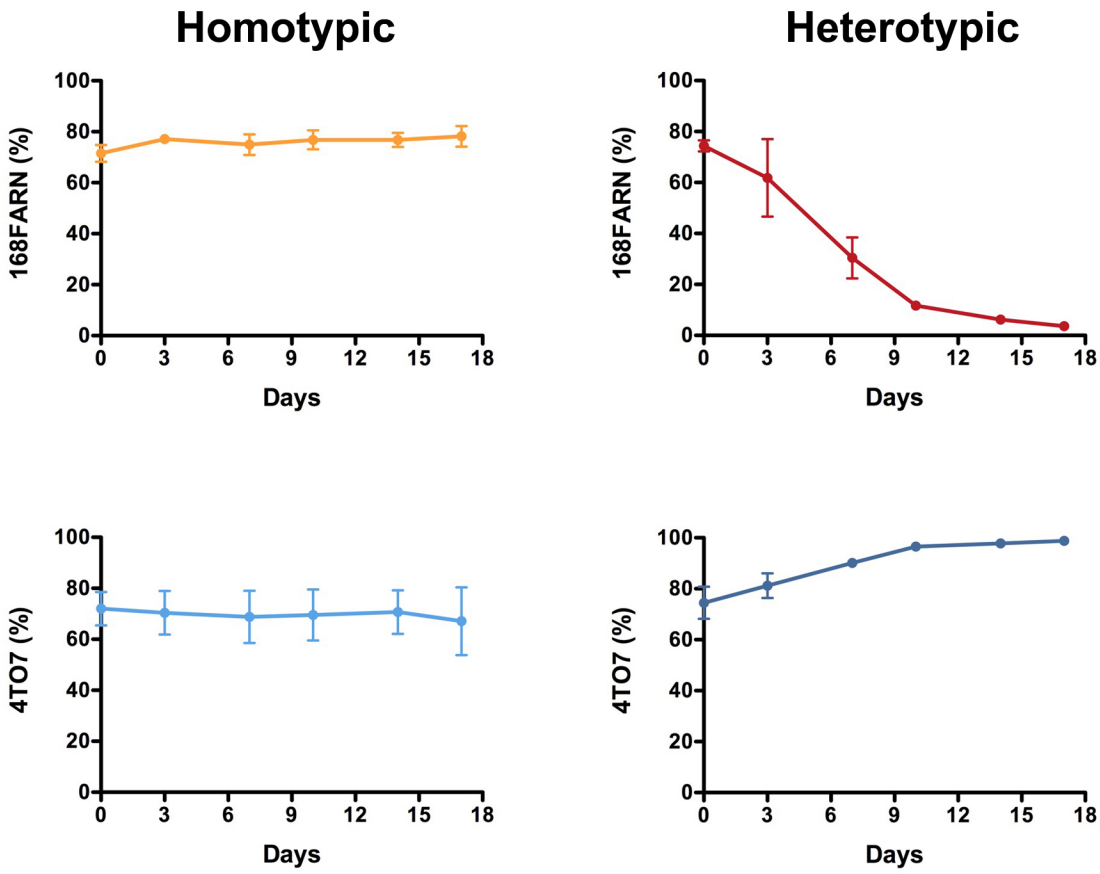

Supplementary Figure 2

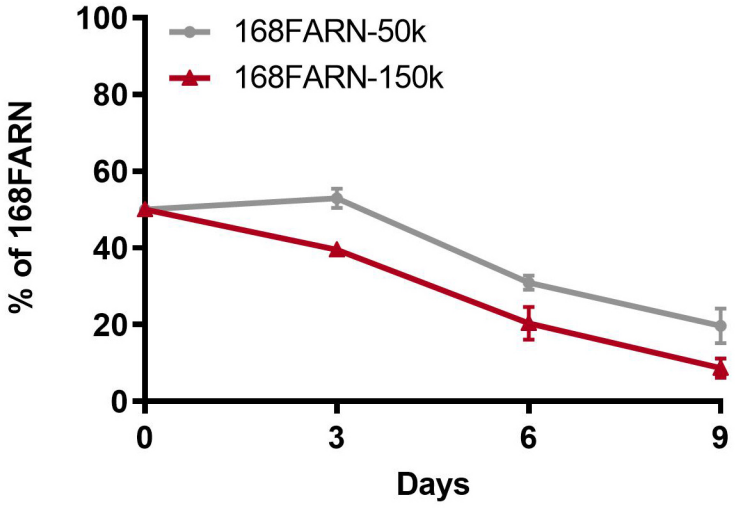

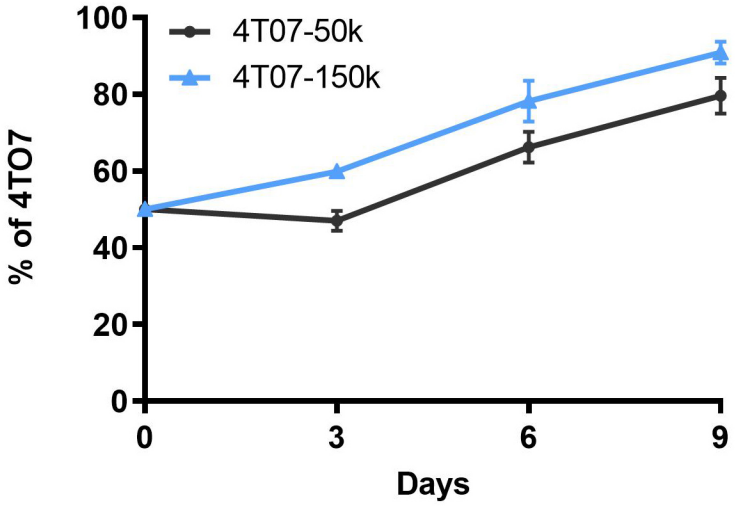

Supplementary Figure 3

A

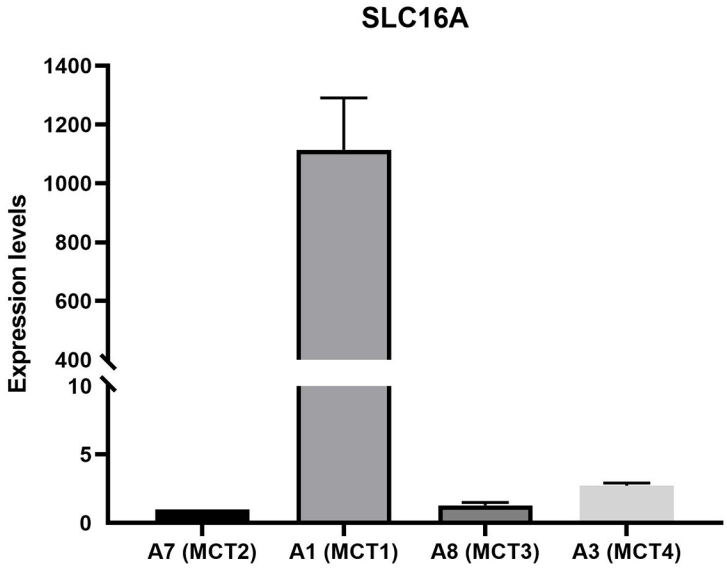

B

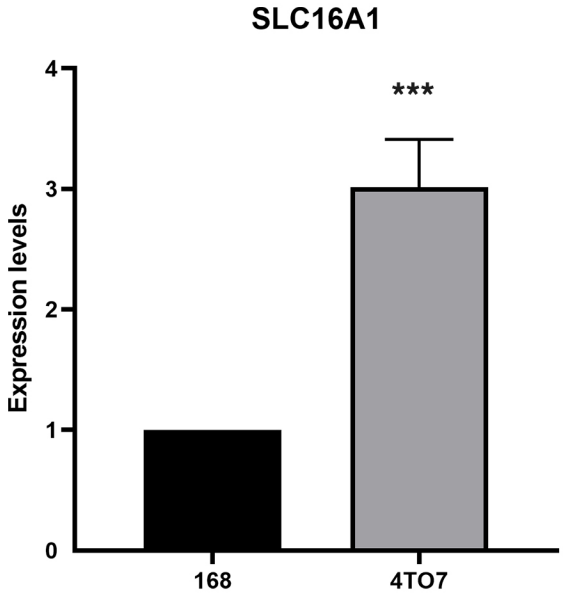
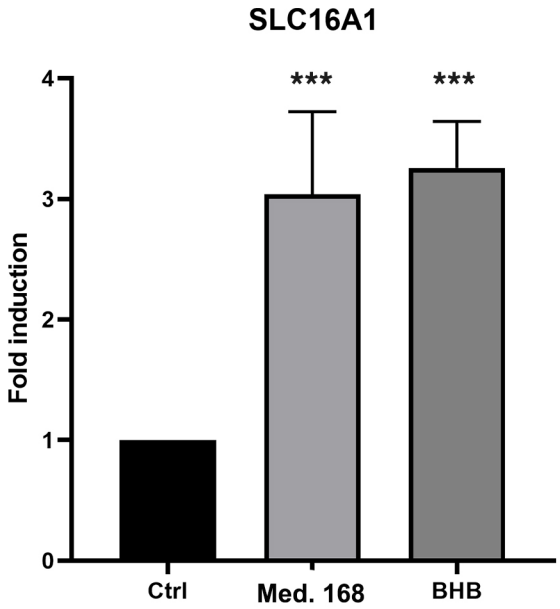
C